University of Groningen

A Two-Step Approach for the Conversion of Technical Lignins to Biofuels

Bernardes Figueiredo, Monique; Venderbosch, Robertus H.; Deuss, Peter; Heeres, Hero

IMPORTANT NOTE: You are advised to consult the publisher's version (publisher's PDF) if you wish to cite from it. Please check the document version below.

Document Version
Publisher's PDF, also known as Version of record

Link to publication in University of Groningen/UMCG research database

FULL PAPER

ADVANCED
SUSTAINABLE
SYSTEMS

www.advsustainsys.com

Check for updates

A Two-Step Approach for the Conversion of Technical Lignins to Biofuels

Monique B. Figueirêdo, Robertus H. Venderbosch, Peter J. Deuss,* and Hero Jan Heeres*

Lignocellulose is a widely available carbon source and a promising feedstock for the production of advanced second-generation biofuels. Nonetheless, lignin, one of its major components, is largely underutilized and only considered an undesired byproduct. Through catalytic hydrotreatment, the highly condensed lignin can be partially depolymerized into a range of monomers. However, its recalcitrance and the presence of aromatic fragments linked by C—C bonds require extensive cracking, which is challenging to achieve. Here, a two-step strategy is reported in which an initial pretreatment step with ozone is used prior to catalytic hydrotreatment to boost lignin depolymerization. Three types of lignin (Kraft, pyrolytic, and Fabiola organosolv) are used as feedstocks and the ozonation step is performed under ambient conditions with either methanol or ethanol as the solvent. The pretreatment is shown to have a positive effect on the subsequent hydrotreatment reaction (Pd/C, 350 °C, 100 bar H_2) and gives product oils with significantly lower M_w (up to 43% lower), higher volatility, and improved calorific values (up to 45.3 MJ kg^{-1}) compared to a direct hydrotreatment.

1. Introduction

The predicted depletion of fossil resources, increase in global energy demand, and pressing environmental concerns related to the use of such resources have encouraged research toward the development of processes to efficiently convert lignocellulosic biomass into second-generation biofuels, biobased chemicals, and performance materials.[1–3] In this context, the lignin fraction (which corresponds to up to 40 wt% of a typical lignocellulosic biomass[4]) is largely underutilized in comparison with the carbohydrate fraction (i.e., cellulose), and for instance, burned for low value energy generation.[5] To fully exploit the potential of biomass as a source of renewable carbon, efficient strategies to valorize lignin are required. Depolymerization of lignin has been shown to have considerable potential,[6] leading to innovative lignin-derived biofuels[7,8] or drop-in chemicals.[9]

In its native form, lignin consists of a highly crosslinked and methoxylated phenylpropanoid network. The structure of the biopolymer changes during isolation in typical (industrial) processes like the Kraft process used in the pulp and paper industry.[10] These technical lignins are currently produced at large scales (e.g., 50 million tons per year of Kraft lignin[11]) and consist of recalcitrant and remarkably complex structures as a result of their processing. Therefore, depolymerization is highly challenging. Various routes have been explored, and some examples are oxidative and reductive treatments using homogeneous and heterogeneous catalysts.[12]

Catalytic hydrotreatment is a well-known reductive upgrading strategy for technical lignins. It involves treatment of lignin with molecular hydrogen (or a hydrogen donor) in the presence of a suitable catalyst. Upon this treatment, hydrodeoxygenation and hydrocracking reactions occur, and a range of valuable monomers can be obtained.[12,13] Interesting results have been reported using different setups, catalysts, reaction conditions, and lignin types (**Table 1**). Nonetheless, the harsh conditions that typically required cause competitive repolymerization that ultimately leads to char in addition to carbon losses to the gas phase. Altogether, these reactions have a negative impact on the techno-economic viability of the process. Furthermore, due to the presence of stable C—C bonds in technical lignins, the yield and quality of the hydrotreated products are yet not optimal for such high end application.[14]

Oxidation strategies have been also reported for lignin depolymerization,[12,33–35] from which ozonation stands as a relatively simple treatment for upgrading technical lignins. Ozone was shown to be highly reactive toward phenolic nuclei and C—C double bonds at ambient conditions, and neither chemical additives nor catalysts are typically required.[36] It can be easily generated in situ either from oxygen or dry air, and such ozone generation technologies are industrially used[37,38] and thus well-established, safe, and available at all scales. Furthermore, ozone has a half-life of <1 h when dissolved,[39] thus any residual ozone in the system quickly decomposes to O_2, providing an overall clean process with no need of extra separation steps.[40] Previous research has shown that the products obtained by ozonation

Dr. M. B. Figueirêdo, Dr. P. J. Deuss, Prof. H. J. Heeres
Department of Chemical Engineering
University of Groningen
Nijenborgh 4, Groningen 9747 AG, The Netherlands
E-mail: p.j.deuss@rug.nl; h.j.heeres@rug.nl
Dr. R. H. Venderbosch
Biomass Technology Group BV
Josink Esweg 34, Enschede 7545 PN, The Netherlands

The ORCID identification number(s) for the author(s) of this article can be found under https://doi.org/10.1002/adsu.201900147.

**ADVANCED
SCIENCE NEWS**

www.advancedsciencenews.com

**ADVANCED
SUSTAINABLE
SYSTEMS**

www.advsustainsys.com

Table 1. Overview of literature data for the catalytic depolymerization of various lignin types.

Lignin feedstock	T [°C]	P_{H_2} [bar]	Catalyst(s)	Ref.
Pyrolytic	340	35	HZSM-5, α-Al$_2$O$_3$, MoO$_3$	[15]
Pyrolytic	230–415	140	CoMo	[16]
Pyrolytic	220–310	190	Ru/C	[17]
Pyrolytic	150–400	69–167	NiMo/Al$_2$O$_3$, Pd/C, Pt/C	[18]
Pyrolytic	300–400	190–200	Ru/C, NiMo/Al$_2$O$_3$	[19]
Pyrolytic	400	100	Ru/C	[20]
Kraft, Alcell, Organosolv, Pyrolytic, Soda	450	100	Limonite	[21]
Kraft	390–450	70–100	Ammonium heptamolybdate	[22]
Kraft, Organocell	400	90–100	Supported NiMo, Cr$_2$O$_3$	[23]
Kraft	350	100	Supported NiMo, CoMo	[24]
Kraft	450	100	Ru, Pt, Pd, and Rh supported in C or Al$_2$O$_3$	[25]
Kraft	350–450	100	Limonite, goethite, iron disulfide, CoMo	[26]
Alcell	400	100	Ru and Pd supported in C, Al$_2$O$_3$, or TiO$_2$, Cu/ZrO$_2$	[27]
Alcell	400	100	Ru/C	[28]
Enzymatic hydrolysis	320–380	40–70	NiMoP/Al$_2$O$_3$	[29]
Enzymatic hydrolysis	195	35	Pd/C	[30]
Organosolv	140–220	0–60	Cu–porous metal oxide	[31]
Soda	350	37	NiMo/Al$_2$O$_3$	[32]

contain a range of oxygenated aromatics, quinones, and carboxylic acids with potential as fuel additives,[40] building blocks for polyurethanes,[41] and as a feed for the synthesis of fine chemicals for the food and pharma industries.[42] Our group has studied the depolymerization of pyrolytic and other technical lignins (i.e., Kraft and organosolv lignins) by ozone into a range of (di)carboxylic acids and esters in detail.[43–45]

As the upgrading potential of technical lignins by direct hydrotreatment is limited, we have explored the potential of an ozone pretreatment to depolymerize the lignin prior to catalytic hydrotreatment. **Figure 1** shows an overview of the proposed strategy (highlighted in the dashed box), which has already shown potential for the upgrading of pyrolysis oils,[46–49] though to the best of our knowledge has not been explored for lignins in general. One interesting aspect of this valorization approach is its potential to be easily incorporated in a hydrogen-based economy. For instance, the development of competitive electrolytic systems for water splitting into green hydrogen gas has gained a lot of attention as a way to decarbonize the global economy, and some scenarios were already shown to be feasible.[50–52] Oxygen gas is the main side product of water splitting (close to 90 wt%) and can be readily transformed to ozone using cheap electricity. Therefore, combining ozone and hydrogen is promising in the context of a hydrogen-based economy relying on the predicted rise of the production of cheap renewable energy.

Thus, we here report a two-step approach for the depolymerization of three technical lignins, i.e., pyrolytic lignin (PL), Kraft lignin (KL), and Fabiola organosolv lignin (OL) using an ozone treatment followed by catalytic hydrotreatment. The lignins were characterized in detail (Section 2.1) and ozonated using ethanol (EtOH) and methanol (MeOH) as the solvents. The ozonated lignin oils were characterized (Section 2.2) and then hydrotreated. Hydrotreatment experiments without an

ozone treatment were also performed to evaluate the potential of the two-step process over direct hydrotreatment (Section 2.3). Mass balance calculations are provided and discussed to highlight the advantages of the proposed two-step strategy (Section 2.4), and possible applications for the product are proposed.

2. Results and Discussion

2.1. Characterization of the Lignin Feedstocks

To investigate the potential of the two-step oxidative–reductive processing of lignin residues, three different lignins were selected. These were i) a PL, which is the water insoluble fraction of a pyrolysis oil obtained from fast pyrolysis of pinewood; ii) a KL commercially available as Indulin-AT which is obtained from pine paper mill black liquor following several cleaning steps; and iii) an OL, in this case a sample from the Fabiola process based on an acetone extraction of beech wood. The three lignin feeds used in this study were characterized in detail by gel permeation chromatography (GPC), thermogravimetric analyses (TGA), ^{13}C-NMR, NMR heteronuclear single quantum coherence (HSQC), and elemental analysis (**Table 2**). The lignins are very different in terms of structure and properties. For instance, the PL shows a much lower M_w and higher volatility in comparison with KL and OL. This is expected due to thermally driven cracking reactions taking place during pyrolysis (500 °C),[53] leading to new aliphatic C—H bonds and significantly lower amounts of methoxy groups bonded to the aromatic backbone (as shown by the ^{13}C-NMR integration results in Table 2). Furthermore, NMR results show that the PL has a much higher proportion of p-hydroxyphenyl (H) units and lacks C—O interunit linkages present in native lignin
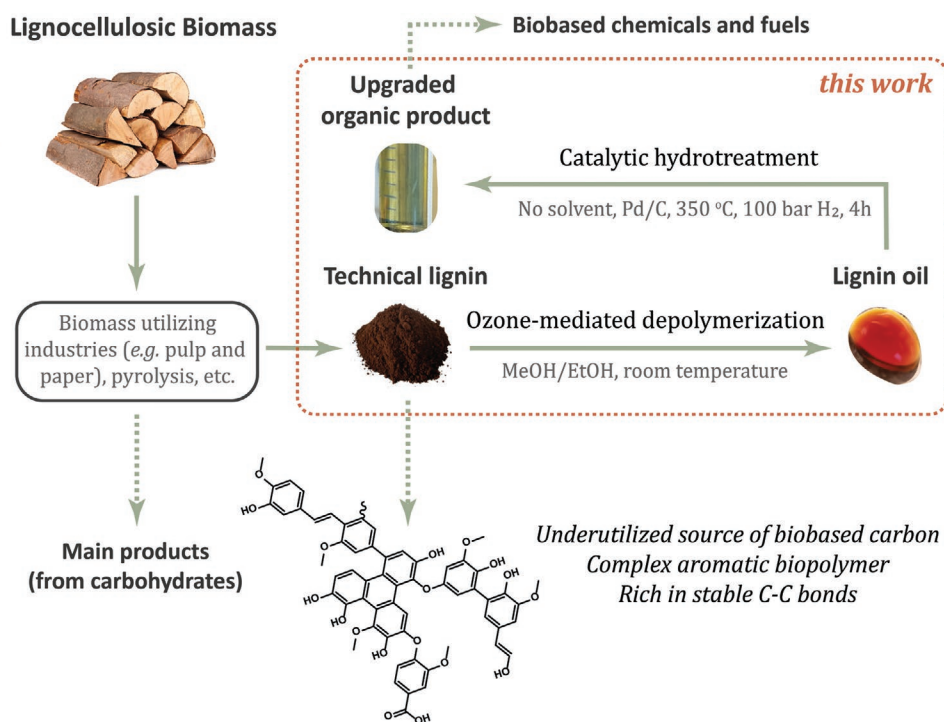
Figure 1. Scheme of the approach proposed for the valorization of technical lignins.

(i.e., β−O−4, β−5, and β−β), again the result of thermally induced depolymerization reactions. The high sulfur content of the KL is a result of the sodium sulfide (Na_2S) used in the

Kraft process, which leads to sulfur incorporation within the lignin structure.[54,55] The KL is obtained from softwood and, as expected, shows a high content of guaiacol (G) units. The OL is

Table 2. Relevant properties of the lignins used in this study.

Property	KL	PL	OL
M_w [g mol^{-1}]	1210	605	1685
TGA residue [wt%]	38.9	16.2	27.3
Elemental composition [wt%] (dry basis)			
C	62.2	63.3	63.42
H	6.00	6.6	5.87
N	0.75	0.0	0.06
O	29.80	30.1	30.61
S	1.20	0.0	0.05
Aliphatic C−H[a] [area%]	13.1	24.1	3.9
Aliphatic C−O[a] [area%]	18.2	14.6	10.5
Aromatic −OCH$_3$[a] [area%]	12.7	7.4	32
Aromatic C−H[a] [area%]	29.5	30.5	28.9
Aromatic C−C[a] [area%]	14.9	14.8	18.8
Aromatic C−O[a] [area%]	10.4	8.2	5.9
Carbonyl[a] [area%]	1.2	0.4	0
S/G/H ratio[b] [%]	0/97.5/2.5	0/52.6/47.4	68.9/30.5/0.5
β−O−4 linkages[b] [%]	10.6	–	19.5
β−5 linkages[b] [%]	2.2	–	3.8
β−β linkages[b] [%]	4.1	–	10.5

[a]As determined by ^{13}C-NMR, refer to the Supporting Information for details; [b]As determined by NMR HSQC, refer to the Supporting Information for details.

**ADVANCED
SCIENCE NEWS**

www.advancedsciencenews.com

**ADVANCED
SUSTAINABLE
SYSTEMS**

www.advsustainsys.com

from a hardwood and thus contains higher amounts of syringol (S) units.[56]

Both KL and PL contain linkages with C—C double bonds (i.e., stilbene linkages), which are likely formed by dehydration and/or formaldehyde elimination reactions.[57–59] On the other hand, the OL used in this study is less degraded due to the relatively mild conditions used in the organosolv extraction process.[60] This is indicated by the higher amounts of C—O interunit linkages (i.e., β—O—4, β—5, and β—β), methoxy groups, and aromatic C—C bonds, which together resemble the native lignin structure to a large extent.

2.2. Lignin Ozonation

All three lignins were exposed to ozone under ambient conditions with both MeOH and EtOH as solvents. KL and OL have low to medium solubility in MeOH and EtOH, and were used as a slurry. The relatively higher solubility of KL in MeOH has been previously reported and is related to the higher hydrogen-bonding capacity and smaller molar volume of MeOH compared to EtOH.[61] KL is also known to be soluble in 1,4-dioxane,[62] and as such this combination was also included in the scope. The products after filtration (for KL and OL) were obtained as low viscous liquids with a reddish color. Interestingly, ozonation leads to a significant increase in solubility of the KL and OL lignin when using alcohols as solvent (i.e., 40–63 wt% of solubilized lignin). The incorporation ratio (IR) factors (i.e., the ratios between lignin oil and dissolved lignin) overall varied between 1.33 and 1.91, indicating a significant mass incorporation (both by oxygen from ozone and solvent participation). Accordingly, a representative elemental analysis of the KL lignin oil (ozonated with EtOH) shows an oxygen content increase from 29.8 wt% (before reaction) to 40.5 wt%. The lower IR factors and acid content of the lignin oils from PL are likely related to the shorter ozonation times applied in this case. This shorter reaction time was selected as ozonation was not necessary for solvation and longer exposure time was previously shown to lead to significant carbon losses as CO_2.[43]

The data in **Table 3** clearly show that the lignin oils have a much lower M_w compared to the corresponding lignin feeds, confirming that lignin depolymerization into soluble fragments occurs to a large extent. This leads to an increase in volatility, as indicated by the lower TGA residue of the lignin oils. High-performance liquid chromatography (HPLC) analyses show the formation of a wide range of low M_w (di)carboxylic acids, corresponding up to 24.2 wt% of the lignin oil. This is expected based on previous ozonation studies, which showed that aromatic ring-opening reactions occur to a large extent during ozonation.[42,43] Solvent reactivity is suggested by variations in the product distribution depending on the solvent used, i.e., higher amounts of acetic acid when using EtOH (see Figure S5 in the Supporting Information). This indicates that a fraction of the produced formic and acetic acids is derived from solvent oxidation (sum < 4 wt%, estimated by blank reactions without lignin). Representative gas chromatography–mass spectrometry (GC–MS) chromatograms of the lignin oils from PL show the formation of methyl esters when using MeOH and ethyl esters when using EtOH (see Figure S6 in the Supporting Information), implying that subsequent esterification reactions occur and lead to the formation of (di)esters.[40,43,63] Products obtained from KL ozonation using 1,4-dioxane show an overall lower amount of low M_w acids and ester when compared to MeOH and EtOH (Table 3). It is unclear if this is solely the result of the different reactivity of these solvents or if it relates to losses during product work-up (as 1,4-dioxane has a higher boiling point than MeOH and EtOH).

HSQC NMR analyses provided insights in structural transformations taking place during ozonation (see Figure S7 in the Supporting Information for representative spectra before and after ozonation). In line with previous studies,[43,64,65] the lignin oils have a more aliphatic character due to ring-opening reactions. In addition, signals related to interunit linkages (i.e., β—O—4, β—β, and β—5) have disappeared. Furthermore, strong signals in regions related to ester and ketone groups can be identified. In conclusion, the depolymerization of the lignins by exposure to ozone was successfully achieved and

Table 3. Ozonation results and relevant properties of the lignin oils.

Property	KL (MeOH)[a]	KL (EtOH)[a]	KL (Diox)[a]	PL (MeOH)[b]	PL (EtOH)[b]	OL (MeOH)[a]	OL (EtOH)[a]
Insoluble lignin before ozonation [wt%]	57	96	0	0	0	85	83
Insoluble lignin after ozonation [wt%]	52	60	0	0	0	54	37
IR [–]	1.83	1.83	1.64	1.55	1.33	1.64	1.91
M_w [g mol^{-1}]	620	635	520	385	400	585	610
M_w decrease[c] [%]	49	47	57	36	34	65	64
TGA residue [wt%]	9.3	15.0	7.3	10.6	11.3	7.4	11.5
Total acids/esters[d] [wt%]	24.2	22.8	13.8	7.9	10.2	23.5	18.6

[a]20 g lignin + 200 g solvent, ozonation performed for 2h, flow of 9.5 g O_3 h^{-1}; [b]20 g lignin + 50 g solvent, ozonation performed for 45 min, flow of 9.5 g O_3 h^{-1}; [c]Based on the M_w of each respective lignin feedstock; [d]See Figure S5 in the Supporting Information for the detailed distribution of the (di)acids identified by HPLC under hydrolysis conditions.

**ADVANCED
SCIENCE NEWS**
www.advancedsciencenews.com

**ADVANCED
SUSTAINABLE
SYSTEMS**
www.advsustainsys.com

the product oils were used for subsequent hydrotreatment experiments.

2.3. Catalytic Hydrotreatment of the (Ozonated) Lignins

The lignin oils obtained after ozonation were subjected to catalytic hydrotreatment for further depolymerization and to remove undesired oxygen-containing chemical functionalities.[66,67] Preliminary experiments were performed with the ozonated KL lignin oil using Pd/C at 350, 375, and 400 °C, a fixed hydrogen pressure of 100 bar and no solvent (see Figure S8 in the Supporting Information). These conditions were selected based on literature data for lignin and pyrolysis oil hydrotreatment (vide supra, Table 1). The temperature has a clear effect on the product oil yield and major carbon losses to gas phase components were observed at higher temperatures, being the result of extensive decarboxylation reactions. For instance, from 350 to 375 and 400 °C, the CO_2 formation increased from 13 to 18 and 21 wt% respectively (based on lignin oil intake). As such, 350 °C was selected for further studies. In addition, the lignins without ozone pretreatment were also hydrotreated under the same conditions to assess the effect of the ozone pretreatment.

Upon hydrotreatment, four distinct product phases were obtained, a solid phase, a gas phase, and two liquid phases (i.e., a light-colored organic and an aqueous phase). **Figure 2** shows the product distribution of the hydrotreatment experiments. Mass balance closures were overall satisfactorily to good (>85%), except for the experiment with the KL lignin oil (MeOH), in which losses during the workup or leakages in the reactor might have led to a slightly lower mass balance closure.

By comparing the product distribution based on the (ozonated) lignin intake, substantial differences in the product distribution are observed when using the lignin oils (i.e., pretreated with ozone) as feedstock compared to the parent lignins. For instance, more aqueous phase is formed via hydrodeoxygenation reactions due to the higher oxygen content of the ozonated lignin oils. Alternatively, the product distribution can be compared based on initial lignin intake before ozonation with and without considering the solvent incorporation (Figures S9 and S10, Supporting Information). It is clear that
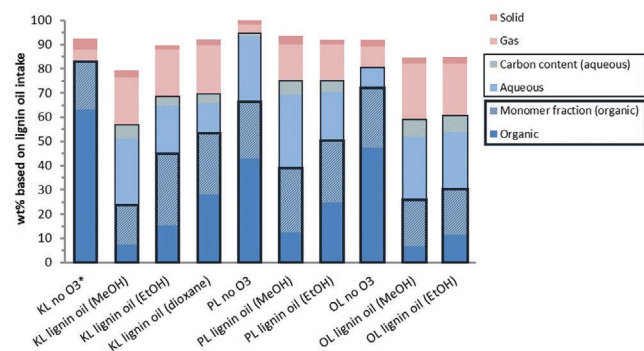
both the amount of lignin being solubilized during ozonation and solvent incorporation strongly influence the product yields and distributions after hydrotreatment. For instance, when the lignin is fully soluble before ozonation (i.e., PL and KL with 1,4-dioxane), this leads to much higher yields based on initial lignin (Figure S9, Supporting Information). Remarkably, when the very tentative assumption is made that the organic monomers are mostly derived from the initial aromatic lignin feedstock (see more detailed analysis of the monomer fraction below) and not from solvent incorporation, their relative yield based on the lignin is increased by 45–110% for the two-step approach compared to direct hydrotreatment (see Figure S10 in the Supporting Information).

Results from total organic carbon (TOC) analyses showed that the aqueous phases from the two-step process have a higher carbon content. This is likely due to the presence of low M_w, water-soluble compounds in the ozonated oils that are resistant to hydrotreatment and thus end up in the aqueous phase. To identify such compounds, an extraction with dichloromethane (DCM) was performed with the aqueous phases obtained from the hydrotreatment of PL and its lignin oils. Most of the organic compounds were extracted to the DCM phase, as shown by the low carbon content of the aqueous phases after extraction (see Figure S11 in the Supporting Information). GC–MS analyses of the extracted DCM phase clearly showed small acids and alcohols such as acetic acid and 1,2-ethanediol (Figure S12, Supporting Information). The lignin oils ozonated in MeOH yielded higher amounts of an aqueous phase after hydrotreatment compared to lignin oils ozonated with EtOH. This is likely a combination of the extent of deoxygenation during hydrotreatment and the extent of esterification during the ozonation step, since water is a product of esterification. The solvent removal step after the ozonation may also remove part of the produced water (particularly when using EtOH due to its higher boiling point), thus affecting the yields of aqueous phase. In addition, the amounts of polar compounds that end up in the aqueous fraction have an impact as well. The higher yields of organic products when using EtOH in the ozonation might be related to the incorporation of ethoxy groups, which are heavier than the methoxy groups incorporated when using MeOH.

Upon hydrotreatment, the proportion of monomers in the organic phase of the ozonated lignins increased compared to those of the untreated lignins. For instance, up to 45 wt%
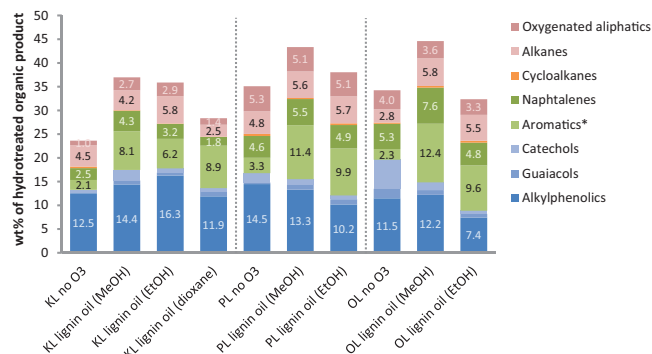

Figure 2. Product distribution after the catalytic hydrotreatment of the lignin feedstocks and their lignin oils. Applied conditions: Pd/C, 350 °C, 100 bar H_2, 1000 RPM, and 4 h (* the direct hydrotreatment of KL yielded a viscous paste instead of a free flowing oil, without the formation of a separate aqueous phase).

Figure 3. Monomer distribution in the hydrotreated organic products, as determined by GC×GC–FID. * Large ester molecules appear in this region.

**ADVANCED
SCIENCE NEWS**
www.advancedsciencenews.com

**ADVANCED
SUSTAINABLE
SYSTEMS**
www.advsustainsys.com

of monomers were estimated by GC×GC–flame ionization detector (FID) in the organic phase (**Figure 3**). General trends on the monomer distribution point out for an increase in alkanes with the ozonation pretreatment. Accordingly, phenolic motifs are highly reactive to ozone, and ring-opening pathways are known to occur,[43,65,68] ultimately leading to the formation of alkanes after deoxygenation. Furthermore, significantly higher amounts of aromatics are observed in the two-step organic products. While this can be a result of the higher reactivity and accessibility of the depolymerized ozonated fragments (leading to a more efficient hydrocracking and hydrodeoxygenation into aromatics), the overlap of large esters in the aromatic region of the chromatogram might play a role. For instance, the lack of a proper separation between these chemical functionalities can cause underestimation of monomers due to the lower response factor of esters. Indeed, GC–MS analyses of the organic products from the two-step approach using PL also showed a range of esters (i.e., methyl esters in the case of MeOH and ethyl esters in the case of EtOH, see Figure S13 in the Supporting Information), confirming that these compounds are more resistant to hydrotreatment in comparison with other chemical functionalities such as phenols.[67,69,70] It is also possible that (poly)alcohols formed during hydroprocessing further follow aromatization pathways,[71–76] however, as detailed mechanistic studies are out of the scope of this work, this could not be confirmed. To better elucidate the main products obtained, GC×GC/time of flight (TOF)-MS analyses were performed with representative samples from PL. In **Figure 4**, a 3D representation of an

organic product from the two-step approach with its main monomers assigned is shown. See Figures S14 and S15 and Table S2 (Supporting Information) for the 2D labeled chromatograms of the organic products from both direct hydrotreatment of PL and the two-step approach. The results clearly show the high amount of esters in the latter, indicating that the amount of esters are likely somewhat underestimated by GC×GC–FID.

When comparing the direct hydrotreatment of the lignins (no O_3 entries in Figure 2, vide supra), large differences are observed regarding product yields due to the structural differences of each lignin. For instance, in the case of KL, no aqueous phase was formed, and the organic product was a very viscous paste. This is in line with previous results reported for KL hydrotreatment at similar conditions,[26] which reported that temperatures higher than 350 °C are required for efficient oxygen removal in the form of water. It also demonstrates that an ozone pretreatment is particularly beneficial for KL hydroprocessing. PL, on the other hand, showed the best direct hydrotreatment results in which a free flowing organic oil (66 wt% yield) and an aqueous phase, together with low amounts of solids and gas, were obtained. This is likely due to its much lower initial M_w and high water content of 11 wt% (estimated by Karl Fischer analysis). The OL yielded a small amount of aqueous phase and a relatively high amount of gas, the latter likely due to the higher amount of methoxy groups present within its hardwood origin (vide supra, Table 1). This was confirmed by the gas compositional analyses that show a higher amount of methane (vide infra).
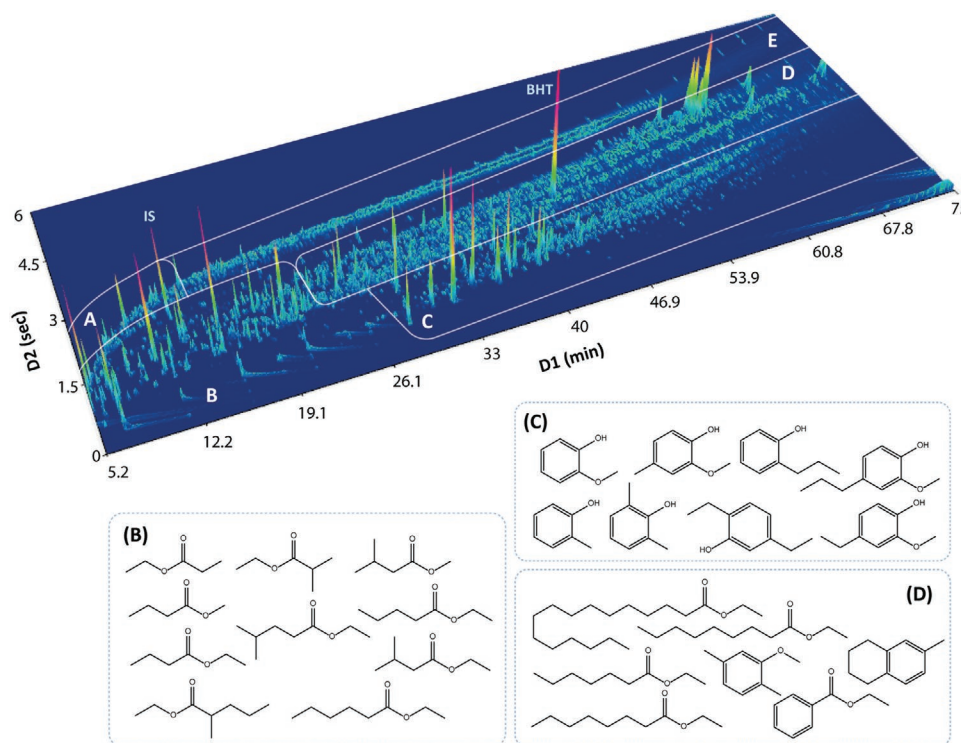

Figure 4. GC×GC/TOF-MS chromatogram of a two-step organic product from PL (EtOH used in the ozonation step) with its main monomers assigned. Region A) contains cycloalkanes; B) oxygenated aliphatics (ketones, esters, acids); C) alkylphenolics; D) aromatics, naphthalenes, large esters; E) alkanes. IS refers to internal standard (DBE) and BHT refers to the stabilizer of the solvent used (THF).
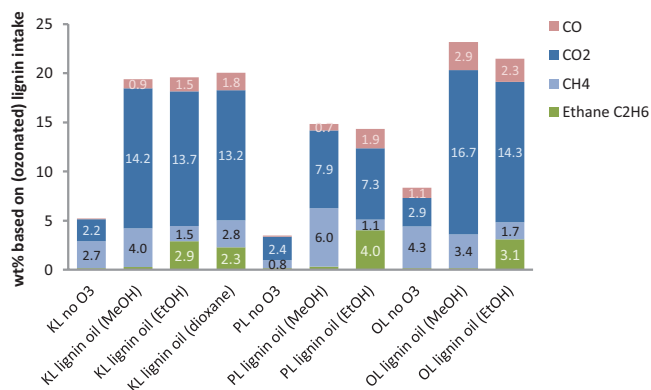
Figure 5. Gas phase composition after catalytic hydrotreatment.

Figure 6. GPC results of the hydrotreated organic products from PL and PL lignin oils.

Overall, no substantial variation in solid formation was observed, yet the gas formation increased substantially in the two-step system. This will be discussed in detail in the following section.

2.3.1. Gas Phase Composition

GC analyses of the gas phases provided important insights regarding structural transformations occurring during ozonation and hydrotreatment of the lignin feedstocks. All experiments were carried at an excess of hydrogen, and at least 61 mol% of the gas phase corresponded to unconverted H_2 (see Figure S16 in the Supporting Information). The main identified gaseous products were methane (CH_4), CO, CO_2, and ethane (C_2H_6), see **Figure 5**. In the case of direct lignin hydrotreatment (i.e., no O_3 entries), the small gas fraction produced (<8.5 wt% based on lignin intake) consisted mainly of CH_4 (from the hydrogenolysis of methoxy substituents present on the lignin structure and/or methanation reactions[77]) and CO_2 (formed by acid-catalyzed decarboxylation reactions of reactive lignin fragments[20,78]). The organosolv lignin yielded higher amounts of CH_4, in line with its higher degree of methoxylation (vide supra, Table 1), as well as CO (which can be formed either by acid-catalyzed decarbonylation or subsequent chemistry in the gas phase, e.g., the reverse water–gas shift reaction[79]).

The amounts of gaseous products increased significantly in the two-step approach, reaching up to 23.3 wt% (based on lignin intake). In detail, ethane was not observed in the MeOH systems, suggesting that it originates from the ethoxy groups formed due to EtOH incorporation during ozonation. In a similar fashion, the MeOH systems showed increased amounts of methane. The use of 1,4-dioxane also led to the formation of ethane, which is likely due to hydrotreatment of residual 1,4-dioxane in the ozonated lignin oil. The higher amounts of CO and particularly of CO_2 confirm the presence of larger amounts of carbonyl and carboxyl functionalities in the ozonated lignin oils, which are a result of acid and ester formation during ozonation. These observations show that the gaseous products formed on the two-step system originate mostly from chemical functionalities formed during the first (ozonation) step. In addition, the formation of gaseous alkanes is directly related to the solvent used in the ozonation
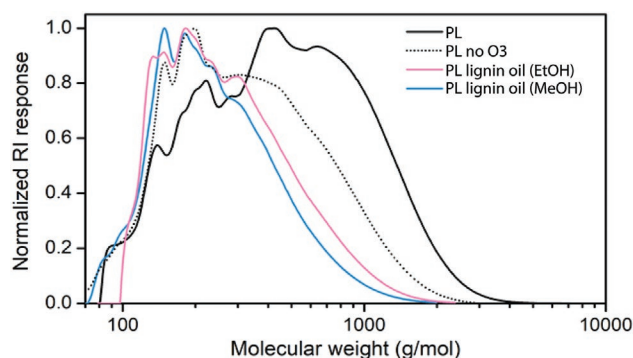
step, as part of it incorporates in the lignin oils (i.e., methoxy and ethoxy groups for MeOH and EtOH, respectively).

2.3.2. Characterization of the Hydrotreated Organic Product Oil

The organic product oils obtained after both direct hydrotreatment and two-step approach were analyzed in detail to assess the extent of hydrodeoxygenation and depolymerization in each case. Accordingly, results from GPC analyses clearly show the differences in molecular weight between the organic products from direct hydrotreatment and the organic products from the two-step system, the latter being significantly more depolymerized (see **Figure 6** for PL results and Figure S17 in the Supporting Information for KL and OL results). The KL results showed the largest difference, as the average M_w decreased up to 43% more in comparison with the direct hydrotreatment (**Figure 7**). These were followed by the PL results (22% lower M_w) and then organosolv results (6% lower M_w). The use of either MeOH or EtOH in the ozonation step did not change the molecular weight distribution substantially. In the case of KL, the use of 1,4-dioxane during ozonation also led to a higher degree of depolymerization when compared to the direct hydrotreatment, but not as substantial as with the alcohols.
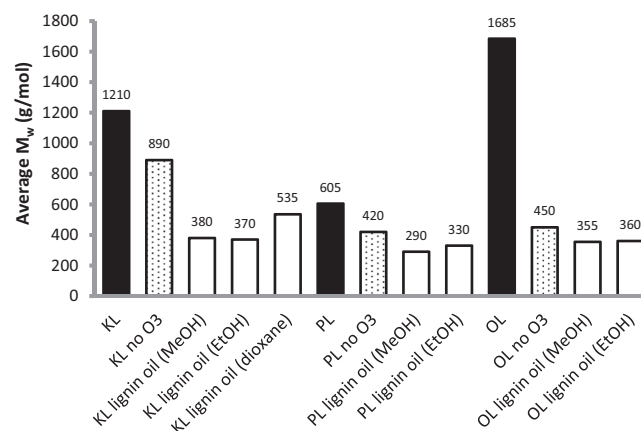

Figure 7. Average M_w (obtained through GPC) of the lignin feeds and their organic products.

**ADVANCED
SCIENCE NEWS**

www.advancedsciencenews.com

**ADVANCED
SUSTAINABLE
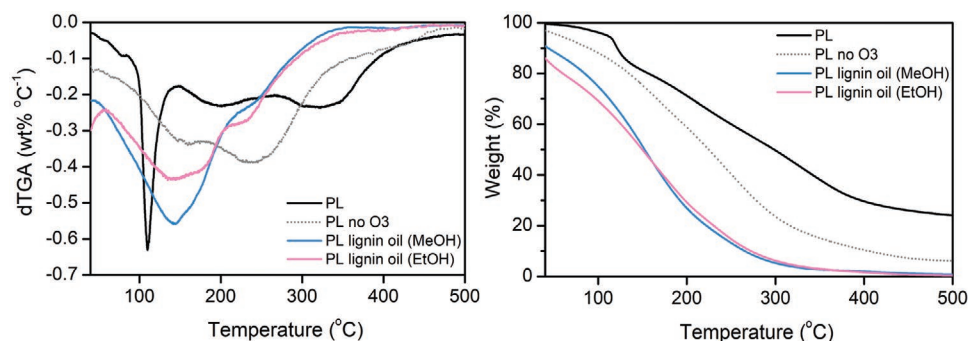SYSTEMS**

www.advsustainsys.com

Figure 8. Representative TGA and TGA derivative curves of the organic products from the hydrotreatment of PL and PL lignin oils.

In line with GPC, representative TGA results of PL also show that the two-step organic products have an overall significantly higher volatility due to the larger extent of depolymerization (**Figure 8**). The high extent of depolymerization, low volatility, and high concentration of esters in the organic products obtained using the proposed the two-step approach are of great interest for biofuel applications.

NMR analyses were performed to provide structural information on the higher molecular weight fraction of the organic products, which cannot be observed by GC techniques. For instance, by integrating the ^{13}C-NMR regions related to specific bonds, further insights in the transformations could be obtained (see Figure S18 in the Supporting Information). Through direct hydrotreatment (i.e., no O_3 entries), aliphatic C—O bonds decreased substantially and aliphatic C—H bonds increased. This is in line with the occurrence of hydrodeoxygenation and hydrocracking. Furthermore, the reactive methoxy groups bonded to the aromatic backbone are removed (mostly in the form of gas, vide supra). The organic products from the two-step system showed an overall increase in aliphatic C—H bonds and decrease in aromatics compared with direct hydrotreatment due to the ring-opening reactions taking place during ozonation.[43] Aliphatic C—O bonds also increased, being mainly related to the formation of esters, which are resistant to hydrotreatment and were identified by GC analysis of the organic products (vide supra). Important to mention, the organic products from the two-step system still show a significant aromatic content (35.6–52.9 area%), which can be desirable due to the various high end possible applications of lignin-derived aromatics and phenolics.[6,8,12]
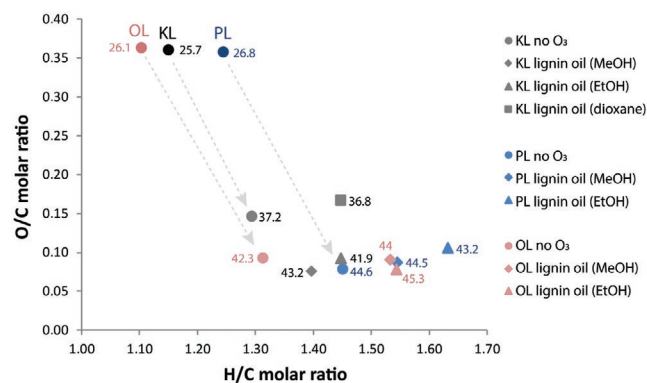
Finally, elemental analysis results provided an overview of the composition of the organic products. In the Van Krevelen plot presented in **Figure 9**, the arrows indicate the transformations caused by the direct hydrotreatment of the three lignin feedstocks, and the label in each datapoint corresponds to the estimated higher heating value (HHV, in MJ kg^{-1}) according to a predictive model based on the elemental composition.[80] In line with the absence of aqueous phase in the direct hydrotreatment of KL (vide supra), its organic product shows a relatively higher O/C ratio compared to products from the direct hydrotreatment of PL and OL. Nonetheless, the oxygen content decreased for all lignin feedstocks, while the H/C ratios increased due to hydrogenation and hydrocracking reactions. For the lignins pretreated with ozone, it was positive to observe that an efficient removal of the added oxygen could be achieved, confirming that the lignin oils had a more accessible structure for hydrotreatment. Furthermore, the fact that oxygen-containing compounds ended up in the aqueous phase after hydrotreatment lowered the O/C molar ratio of the final organic product. The H/C molar ratios increased due to incorporation of alkyl chains from the solvents and the higher depolymerization achieved in the two-step system (vide supra). In the case of KL, the oils pretreated with both MeOH and EtOH had a remarkably higher quality, and the HHV increased by around 20% compared to the organic product from direct hydrotreatment. The organic product from the 1,4-dioxane system showed a higher oxygen content and therefore lowered HHV, suggesting that, despite the advantageous full solubility of KL leading to higher yields, this solvent is not adequate for the proposed strategy. Other disadvantages worth mentioning are related to the fossil-based character and higher toxicity of 1,4-dioxane when compared to MeOH and EtOH. In the case of KL and OL systems, which have a drawback related to the low initial solubility of the feedstocks in MeOH and EtOH, it is expected that optimized ozonation setups with proper attention to mass transfer issues lead to higher yields of dissolved lignin.[45] In the case of PL, the estimated HHV did not vary significantly between organic products, and all values are high and similar to those of traditional petro-based fuels.[81] Overall, the organic products from the two-step system have enhanced properties for biofuel applications. In detail, the full solubility of PL in both MeOH and EtOH leading to higher yields and facilitating the process' operation, as well as the high volatility and degree of depolymerization of the PL-derived organic products (vide supra) indicates great potential for the straightforward use of this lignin

Figure 9. Van Krevelen plot of the lignin feedstocks, their organic products, and estimated HHV values (in MJ kg^{-1}).

type as feedstock in multistep upgrading strategies. Following the results presented, the next section discusses an overall mass balance of the proposed two-step strategy using PL as reference.

2.4. Overall Mass Balances

The previous sections showed the improved properties of the organic products for the two-step approach compared to a direct hydrotreatment of lignin, i.e., lower M_w, higher volatility, and higher monomer yields. However, overall mass balances taking the solvent incorporation into account should be considered to assess the potential of the two-step approach. The results obtained using PL were selected for a deeper analysis due to the promising results observed and the full solubility of PL in both MeOH and EtOH, which led to higher yields of monomers in the organic products (vide supra). Interestingly, the hydrogen consumption was higher in the direct hydrotreatment of PL (408 nL H_2 kg^{-1}) in comparison with the hydrotreatment of the PL lignin oils (313–331 nL H_2 kg^{-1}). This is likely related to the fact that esters and acids formed during ozonation are more resistant to hydrotreatment. While the former is of interest for biofuel applications, the latter ends up in the aqueous phase and can be used for other applications or further processed. Due to the high costs of hydrogen, a lower consumption is beneficial for the overall process' feasibility.

Figure 10 shows the overall mass balances of the direct hydrotreatment of PL and the two-step approach using both MeOH and EtOH. While the organic yields were similar (but

slightly lower when using MeOH), an overall increase of 10–12 wt% in the organic monomer yields is observed in the two-step approach. Furthermore, a significant increase in the amounts of water-soluble monomers (i.e., up to 5 times higher) and gaseous alkanes (i.e., 7–10 times higher) is observed. While aqueous streams can be further reformed to yield light alkanes and hydrogen,[82,83] the gaseous alkanes produced can be used to generate power to the process, and the solvent used in the ozonation step can be recycled, as well as the large fraction of unreacted hydrogen after hydrotreatment (represented by dashed arrows in the figure).

This overview aims to shed light on the potential of the novel oxidative–reductive concept here presented to convert technical lignins into added-value streams, and how these streams can be possibly integrated and recycled. There are many opportunities for optimization, e.g., use of different solvents, reaction times, and ozone concentration in the ozonation step. The use of continuous setups can be highly advantageous for a more efficient use of ozone while suppressing overoxidation (thus, carbon losses to CO_2).[45] With respect to the hydrotreatment step, reaction conditions and type of catalyst can tune product distribution and possibly shift results toward higher organic yields and lower costs. Some important aspects observed have a positive impact on the techno-economic viability of the two-step concept. For instance, the hydrogen consumption, an important variable cost contributor, was actually lower for the two-step systems in comparison with the direct hydrotreatment. Furthermore, both ozone and hydrogen are expected to become much cheaper and available by the anticipated reduction of global electricity prices
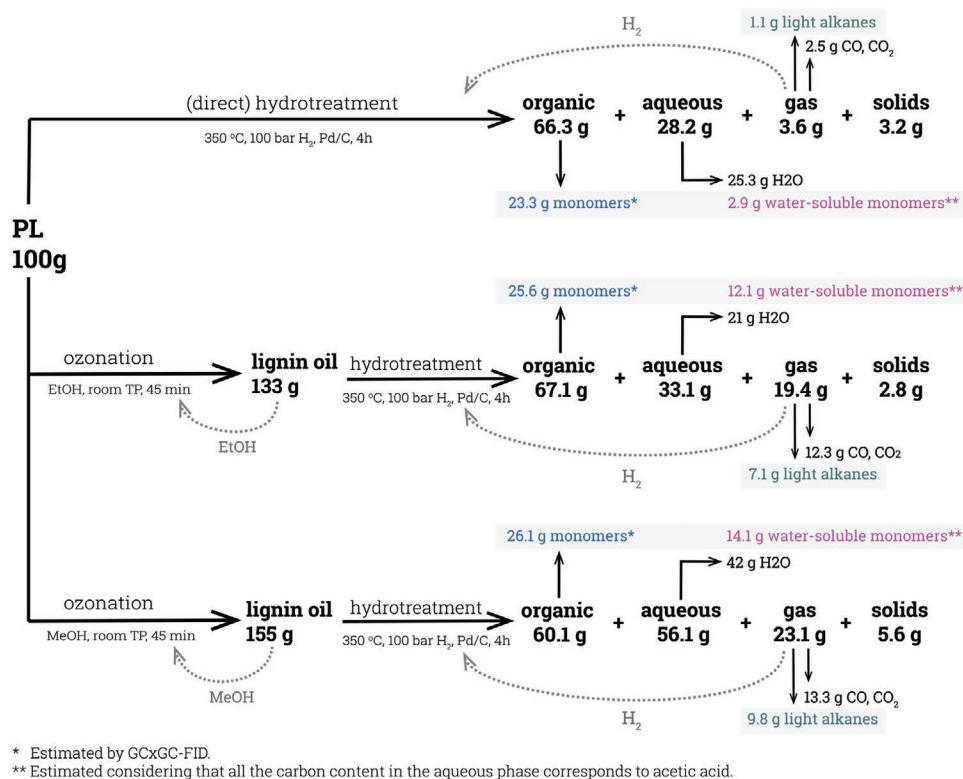

* Estimated by GCxGC-FID.
** Estimated considering that all the carbon content in the aqueous phase corresponds to acetic acid.

Figure 10. Overall mass balances for PL (direct hydrotreatment and two-step systems).

due to the ever increasing amount of electricity generated by renewable resources and the current developments toward a hydrogen-based economy. Accordingly, the electrolysis of water with cheap electricity produces hydrogen and oxygen, and the latter can be converted to ozone (using again cheap electricity). Such future perspectives endorse the potential of the process here described for the upgrading of technical lignins that arise as residues from biomass processing.

3. Conclusions

In this work, we report a two-step oxidative–reductive system that is able to convert technical lignins into products with enhanced biofuel properties. Three lignin types (i.e., KL, PL, and OL) were used as feedstocks, and the oxidative step was performed under ambient conditions using ozone and either MeOH, EtOH, or 1,4-dioxane as the solvent. Such straightforward ozonation step effectively depolymerized the lignin feedstocks into lignin oils, which were hydrotreated after solvent removal. The pretreatment was shown to improve the product properties of a subsequent relatively mild catalytic hydrotreatment (Pd/C, 350 °C, 100 bar H_2), yielding equivalent yields of organic mixtures with significantly lower M_w (up to 43% lower), higher volatility, improved calorific values (up to 45.3 MJ kg^{-1}), and higher monomer yields (i.e., 10–12 wt% higher in the case of PL). In addition, higher amounts of water-soluble monomers were produced in the two-step systems, and these could be easily extracted. Apart from MeOH, it was shown that EtOH was also suitable for the process, being highly advantageous due to its biobased character and low toxicity. These solvents also had a significant influence on the observed gaseous products (i.e., methane or ethane), acids (i.e., formic or acetic acid), and ester products (i.e., methyl or ethyl esters) due to their participation in some reaction pathways. Ring-opening reactions during the ozone pretreatment led to the formation of esters and acids, and most of the acids ended up in the aqueous phase. This resulted in a lower hydrogen consumption during hydrotreatment, being advantageous due to the high costs associated with hydrogen. The efficient removal of the oxygen in the second step shows the great accessibility of the lignin oil's structure, highlighting the potential of the two-step strategy on improving the hydroprocessing of recalcitrant lignin residues, ultimately leading to products with enhanced properties and great potential for biofuel applications. There are several opportunities for process optimization aiming for lower carbon losses (which were shown to be largely derived from solvent incorporation) and higher yields in the case of insoluble lignins such as KL and OL, e.g., evaluation of other solvents and ozonation conditions, use of setups with improved mass transfer to maximize the yields of dissolved lignin, use of cheaper catalysts and milder conditions in the hydrotreatment step. Finally, due to the current developments toward a green hydrogen economy, costs related to electricity and the production of the main reagents of the process here evaluated (H_2 and O_3) are expected to drop. We believe that this promising future perspective will support further developments in the field of lignin valorization using a combination of ozone and hydrogen.

4. Experimental Section

Chemicals: Pine-derived pyrolysis oil was supplied by BTG (Biomass Technology Group B.V., Enschede, the Netherlands) and produced at 500 °C in a rotating cone reactor[84] (capacity of 5 kg h^{-1}, typical residence time < 2 s). The PL fraction was obtained by the application of water washings on the pyrolysis oil (see the Supporting Information for the detailed procedure). Indulin-AT KL was supplied by MeadWestvaco Specialty Chemicals, USA. Indulin-AT is a purified form of pine-derived KL and does not contain residual sugars. Fabiola acetosolv lignin (OL) from beech wood was kindly provided by TNO. The synthesis procedure for the latter is described elsewhere.[60] KL and OL were obtained in powder form, while the PL was obtained as a viscous dark brown liquid. The Pd/C catalyst (powder) was from Sigma-Aldrich and contained 5 wt% of active metal. The average metal nanoparticle size was 2.9 nm (determined by transmission electron microscopy, Figure S1 (Supporting Information)) and the surface area was 1025 m^2 g^{-1} (determined by Brunauer–Emmett–Teller analyses).[85] Tetrahydrofuran (THF), DCM, toluene, EtOH, MeOH, 1,4-dioxane (dioxane), deuterated dimethyl sulfoxide (DMSO-d$_6$), and di-n-butyl ether (DBE) were purchased from Sigma-Aldrich. All these chemicals were used as received.

Ozonation Experiments: The ozonation experiments were performed at ambient conditions and based on a previously published procedure.[43] 20 g of lignin (KL or OL) and 200 g of solvent (EtOH, MeOH, or 1,4-dioxane) were added to a bubble column reactor (Figure S2, Supporting Information). Ozonation was performed for 2 h and ozone was introduced in the reactor by using a dip tube. Ozone was produced by a generator (Model LAB2B from Ozonia) fed by pure oxygen from a cylinder, and the inlet gas flow (ozone diluted in oxygen) was fixed at 4 L min^{-1} (corresponding to 9.5 g O_3 h^{-1}). Ozonation conditions of PL were different due to its complete solubility, relatively depolymerized structure, and foaming behavior in the reactor. In this case, 20 g of PL and 50 g of solvent were used in each experiment, which lasted 45 min (ozone input of 9.5 g O_3 h^{-1}). After reactions with KL or OL, the oxidized mixture was flushed with air for around 2 min to remove residual ozone and filtered to recover solids. As PL is fully soluble in both MeOH and EtOH, no filtration was necessary. The same applied to KL in combination with 1,4-dioxane. The solvent was removed by vacuum evaporation (150 mbar, 45 °C for EtOH; 250 mbar, 45 °C for MeOH; 60 mbar, 45 °C for 1,4-dioxane) to yield the final lignin oil, which was weighted, analyzed in detail, and subsequently hydrotreated.

Since KL and OL have a low solubility in MeOH and EtOH and the mass increases during ozonation (due to incorporation of oxygen from ozone and solvent fragments in the structure, vide infra), the amounts of dissolved lignin were calculated based on the solids recovered after each experiment (here called insoluble lignin). These solids were considered unreacted lignin and provided an indication of how much of the initial lignin was extracted to the solvent after ozonation (i.e., dissolved lignin), see Equations (1) and (2). By knowing the amount of dissolved lignin, the mass incorporation could be quantified as well (Equation (3)). For the reactions performed with 1,4-dioxane and PL, the mass incorporation was calculated directly, as no filtration was needed. For a better comparison between the experiments, an IR factor was also defined (Equation (4)). The reader is referred to the Supporting Information for an example of calculations using the data obtained from a typical ozonation experiment

$$\text{Insoluble lignin} \, (\text{wt\%}) = \frac{\text{Insoluble lignin} \, (\text{g})}{\text{Initial lignin} \, (\text{g})} \times 100 \tag{1}$$

$$\text{Dissolved lignin} = \text{Initial lignin} \, (\text{g}) - \text{Insoluble lignin} \, (\text{g}) \tag{2}$$

$$\text{Mass incorporation} = \text{Lignin oil} \, (\text{g}) - \text{Dissolved lignin} \, (\text{g}) \tag{3}$$

$$\text{Incorporation ratio} \, (\text{IR}) = \frac{\text{Lignin oil} \, (\text{g})}{\text{Dissolved lignin} \, (\text{g})} \tag{4}$$

**ADVANCED
SCIENCE NEWS**
www.advancedsciencenews.com

**ADVANCED
SUSTAINABLE
SYSTEMS**
www.advsustainsys.com

Catalytic Hydrotreatment Experiments: The (ozonated) lignin oils were hydrotreated in a 100 mL batch autoclave (Parr), with the maximum pressure and temperature of 350 bar and 500 °C. The reactor was surrounded by a metal block containing electrical heating elements and channels allowing the flow of cooling water. The reactor content was stirred mechanically at 1000 rpm using a Rushton type turbine with a gas-induced impeller. In a typical experiment, the reactor was charged with 15 g of feed and 0.75 g (i.e., 5 wt% on lignin intake) of catalyst. Subsequently, the reactor was pressurized to 170 bar with hydrogen at room temperature for leak testing, flushed 3 times, and pressurized again to 100 bar. The reactor was heated to 350 °C at a heating rate of around 10 °C min^{-1}, and the reaction time was set at zero when the predetermined temperature was reached. After the predetermined reaction time of 4 h, the reactor was cooled to room temperature at a rate of about 40 °C min^{-1}. The final pressure was recorded for mass balance calculations, and the gas phase was sampled in a gas bag for composition analysis. The product was collected as a slurry and centrifuged (15 min at 4500 RPM) to separate organic phase, aqueous phase, and solids. The separated liquid phases were collected and weighted. The reactor, stirrer, and centrifuge tube with solids (i.e., char + catalyst) were washed with DCM and filtered for an accurate quantification of the solid fraction. DCM was left overnight to evaporate, and the remaining organics after DCM removal were also weighted for an accurate quantification of the oil fraction (see Figure S3 in the Supporting Information for the work-up scheme).

Feed and Lignin Oil Analyses: The properties of the lignin oils and hydrotreated products were assessed by a series of techniques, among others the weight average molecular weight (M_w) and molecular weight distribution (GPC), charring tendency and volatility (TGA), identification of thermally stable monomers (GC×GC-FID, GC×GC/TOF-MS, GC–MS), (di)carboxylic acid identification and quantification (HLPC), structural features (HSQC NMR, ^{13}C-NMR), water content (Karl Fischer analysis), elemental composition (C, H, N, S), and carbon content of the aqueous phase (TOC analysis). Prior to the experiments, the lignin feedstocks were characterized by GPC, TGA, ^{13}C-NMR, HSQC NMR (see Figure S4 in the Supporting Information for assignment), and elemental composition (C, H, N, S).

GPC analyses of the feedstocks and products were performed using an Agilent HPLC 1100 system equipped with a refractive index detector. Three columns in series of MIXED type E (length 300 mm, internal diameter (i.d.) 7.5 mm) were used. Polystyrene standards were used for calibration. 0.05 g of the sample was dissolved in 4 mL of THF together with 2 drops of toluene as the external reference and filtered (filter pore size 0.45 μm) before injection. TGA were performed using a TGA 7 from Perkin-Elmer. The samples were heated under a nitrogen atmosphere (nitrogen flow of 50 mL min^{-1}), with a heating rate of 10 °C min^{-1} and temperature ramp of 30–800 °C. For analysis by GC, samples were diluted around 20 times with a 500 ppm solution of DBE (internal standard) in THF. GC×GC/TOF-MS analysis was performed on an Agilent 7890B system equipped with a JEOL AccuTOF GCv 4G detector and two capillary columns, i.e., a RTX-1701 capillary column (30 m × 0.25 mm i.d. and 0.25 μm film thickness) connected by a solid state modulator (Da Vinci DVLS GC²) to a Rxi-5Sil MS column (120 cm × 0.10 mm i.d. and 0.10 μm film thickness). GC×GC–FID analysis was performed on a trace GC×GC system from Interscience equipped with a cryogenic trap and two capillary columns, i.e., a RTX-1701 capillary column (30 m × 0.25 mm i.d. and 0.25 μm film thickness) connected by a Meltfit to a Rxi-5Sil MS column (120 cm × 0.15 mm i.d. and 0.15 μm film thickness). Quantification of GC×GC main groups of compounds (e.g., aromatics, alkanes, alkylphenolics) was performed by using an average relative response factor per component group in relation to an internal standard (DBE). GC–MS analysis was performed on a Hewlett-Packard 5890 gas chromatograph equipped with a RTX-1701 capillary column (30 m × 0.25 mm i.d. and 0.25 μm film thickness) and a Quadrupole Hewlett-Packard 6890 MSD selective detector attached. Helium was used as carrier gas (flow rate of 2 mL min^{-1}). The injector temperature was set to 280°C. The oven temperature was kept at 40 °C for 5 min, then increased to 250 °C at a rate of 3 °C min^{-1} and held at 250 °C for

5 min. The HPLC analytical device used for carboxylic acid identification and quantification consisted of an Agilent 1200 pump, a Bio-Rad organic acids column Aminex HPX-87H, a Waters 410 differential refractive index detector, and a UV detector. The mobile phase was 5×10^{-3} M aqueous sulfuric acid at a flow rate of 0.55 mL min^{-1}. The HPLC column was operated at 60 °C. Since the products were not fully soluble in water, a water extraction step (proportion of 1:10 of organics and water) was needed, and the aqueous phase was further analyzed. Calibration curves of the targeted acids were built to provide an accurate quantification and were based on a minimum of 4 data points with excellent linear fitting (i.e., $R^2 > 0.99$). NMR experiments were performed on a Bruker NMR spectrometer (600 MHz) at 293 K using a standard 90° pulse, and the spectra were processed and analyzed using MestReNova software, refer to the Supporting Information for integration details. The water content was determined by Karl Fischer titration using a Metrohm 702 SM Titrino titration device. About 0.01 g of sample was injected in an isolated glass chamber containing Hydranal (Karl Fischer solvent, Riedel de Haen). The titrations were carried out using the Karl Fischer titrant Composit 5K (Riedel de Haen). All analyses were performed at least 3 times and the average value was reported. Elemental analysis (C, H, N, S) were performed using a EuroVector EA3400 Series CHNS-O analyzer with acetanilide as the reference. The oxygen content was determined indirectly by difference. All analyses were carried out at least in duplicate and the average value was reported. The TOC in the water phase was measured by using a Shimadzu TOC-VCSH with an OCT-1 sampler port. Prior to analysis, each sample was diluted around 50–100 times in water.

Gas Phase Analysis: The gas phases after catalytic hydrotreatment experiments were collected in a gas bag (SKC Tedlar 3 L sample bag (9.5" × 10")) with a polypropylene septum fitting. GC–thermal conductivity detector analyses were performed using a Hewlett Packard 5890 Series II GC equipped with a Porablot Q Al₂O₃/Na₂SO₄ column and a molecular sieve (5 A) column. The injector temperature was set at 150 °C and the detector temperature at 90 °C. The oven temperature was kept at 40 °C for 2 min, then heated up to 90 °C at 20 °C min^{-1} and kept at this temperature for 2 min. A reference gas (containing 55.19% H₂, 19.70% CH₄, 3.00% CO, 18.10% CO₂, 0.51% ethylene, 1.49% ethane, 0.51% propylene, and 1.50% propane) was used to identify and quantify the gaseous products.

Supporting Information

Supporting Information is available from the Wiley Online Library or from the author.

Conflict of Interest

The authors declare no conflict of interest.

**ADVANCED
SCIENCE NEWS**

www.advancedsciencenews.com

**ADVANCED
SUSTAINABLE
SYSTEMS**

www.advsustainsys.com

[1] S. P. S. Chundawat, G. T. Beckham, M. E. Himmel, B. E. Dale, *Annu. Rev. Chem. Biomol. Eng.* **2011**, *2*, 121.

[2] C.-H. Zhou, X. Xia, C.-X. Lin, D.-S. Tong, J. Beltramini, *Chem. Soc. Rev.* **2011**, *40*, 5588.

[3] F. H. Isikgor, C. Remzi Becer, *Polym. Chem.* **2015**, *6*, 4497.

[4] A. J. Ragauskas, G. T. Beckham, M. J. Biddy, R. Chandra, F. Chen, M. F. Davis, B. H. Davison, R. A. Dixon, P. Gilna, M. Keller, P. Langan, A. K. Naskar, J. N. Saddler, T. J. Tschaplinski, G. A. Tuskan, C. E. Wyman, *Science* **2014**, *344*, 1246843.

[5] R. J. A. Gosselink, E. de Jong, B. Guran, A. Abächerli, *Ind. Crops Prod.* **2004**, *20*, 121.

[6] F. Cheng, C. E. Brewer, *Renewable Sustainable Energy Rev.* **2017**, *72*, 673.

[7] H. Wang, H. Ruan, H. Pei, H. Wang, X. Chen, M. P. Tucker, J. R. Cort, B. Yang, *Green Chem.* **2015**, *17*, 5131.

[8] P. Bi, J. Wang, Y. Zhang, P. Jiang, X. Wu, J. Liu, H. Xue, T. Wang, Q. Li, *Bioresour. Technol.* **2015**, *183*, 10.

[9] Z. Cao, M. Dierks, M. T. Clough, I. B. Daltro de Castro, R. Rinaldi, *Joule* **2018**, *2*, 1118.

[10] S. Constant, H. L. J. Wienk, A. E. Frissen, P. de Peinder, R. Boelens, D. S. van EsR. J. H. Grisel, B. M. Weckhuysen, W. J. J. Huijgen, R. J. A. Gosselink, P. C. A Bruijnincx, *Green Chem.* **2016**, *18*, 2651.

[11] P. C. A. Bruijnincx, R. Rinaldi, B. M. Weckhuysen, *Green Chem.* **2015**, *17*, 4860.

[12] J. Zakzeski, P. C. Bruijnincx, A. L. Jongerius, B. M. Weckhuysen, *Chem. Rev.* **2010**, *110*, 3552.

[13] C. Xu, R. A. D. Arancon, J. Labidi, R. Luque, *Chem. Soc. Rev.* **2014**, *43*, 7485.

[14] M. Li, Y. Pu, A. J. Ragauskas, *Front. Chem.* **2016**, *4*, https://doi.org/10.3389/fchem.2016.00045.

[15] X. Zhang, Q. Chen, Q. Zhang, C. Wang, L. Ma, Y. Xu, *J. Anal. Appl. Pyrolysis* **2018**, *135*, 60.

[16] J. Piskorz, P. Majerski, D. Radlein, D. Scott, *Energy Fuels* **1989**, *3*, 723.

[17] F. de Miguel Mercader, M. J. Groeneveld, S. R. A. Kersten, C. Geantet, G. Toussaint, N. W. J. Way, C. J. Schaverien, K. J. A. Hogendoorn, *Energy Environ. Sci.* **2011**, *4*, 985.

[18] R. J. French, S. K. Black, M. Myers, J. Stunkel, E. Gjersing, K. Iisa, *Energy Fuels* **2015**, *29*, 7985.

[19] S. Kadarwati, S. Oudenhoven, M. Schagen, X. Hu, M. Garcia-Perez, S. Kersten, C.-Z. Li, R. Westerhof, *J. Anal. Appl. Pyrolysis* **2016**, *118*, 136.

[20] A. Kloekhorst, J. Wildschut, H. Jan Heeres, *Catal. Sci. Technol.* **2014**, *4*, 2367.

[21] I. Hita, H. J. Heeres, P. J. Deuss, *Bioresour. Technol.* **2018**, *267*, 93.

[22] A. Oasmaa, A. Johansson, *Energy Fuels* **1993**, *7*, 426.

[23] A. Oasmaa, R. Alén, D. Meier, *Bioresour. Technol.* **1993**, *45*, 189.

[24] C. R. Kumar, N. Anand, A. Kloekhorst, C. Cannilla, G. Bonura, F. Frusteri, K. Barta, H. J. Heeres, *Green Chem.* **2015**, *17*, 4921.

[25] I. Hita, P. J. Deuss, G. Bonura, F. Frusteri, H. J. Heeres, *Fuel Process. Technol.* **2018**, *179*, 143.

[26] S. Agarwal, R. K. Chowdari, I. Hita, H. J. Heeres, *ACS Sustainable Chem. Eng.* **2017**, *5*, 2668.

[27] A. Kloekhorst, H. J. Heeres, *ACS Sustainable Chem. Eng.* **2015**, *3*, 1905.

[28] A. Kloekhorst, H. Jan Heeres, *Catal. Sci. Technol.* **2016**, *6*, 7053.

[29] J. Horáček, F. Homola, I. Kubičková, D. Kubička, *Catal. Today* **2012**, *179*, 191.

[30] K. M. Torr, D. J. van de Pas, E. Cazeils, I. D. Suckling, *Bioresour. Technol.* **2011**, *102*, 7608.

[31] K. Barta, G. R. Warner, E. S. Beach, P. T. Anastas, *Green Chem.* **2014**, *16*, 191.

[32] B. Joffres, C. Lorentz, M. Vidalie, D. Laurenti, A.-A. Quoineaud, N. Charon, A. Daudin, A. Quignard, C. Geantet, *Appl. Catal., B* **2014**, *145*, 167.

[33] H. Lange, S. Decina, C. Crestini, *Eur. Polym. J.* **2013**, *49*, 1151.

[34] C. Crestini, M. Crucianelli, M. Orlandi, R. Saladino, *Catal. Today* **2010**, *156*, 8.

[35] R. Behling, S. Valange, G. Chatel, *Green Chem.* **2016**, *18*, 1839.

[36] R. Ma, Y. Xu, X. Zhang, *ChemSusChem* **2015**, *8*, 24.

[37] Z. B. Guzel-Seydim, A. K. Greene, A. C. Seydim, *LWT – Food Sci. Technol.* **2004**, *37*, 453.

[38] R. G. Rice, *Ozone: Sci. Eng.* **1996**, *18*, 477.

[39] S. T. Oyama, *Catal. Rev.* **2000**, *42*, 279.

[40] C. J. Chuck, H. J. Parker, R. W. Jenkins, J. Donnelly, *Bioresour. Technol.* **2013**, *143*, 549.

[41] Y. Zhang, R. Yan, T. Ngo, Q. Zhao, J. Duan, X. Du, Y. Wang, B. Liu, Z. Sun, W. Hu, H. Xie, *Eur. Polym. J.* **2019**, *117*, 114.

[42] R. Ma, M. Guo, X. Zhang, *ChemSusChem* **2014**, *7*, 412.

[43] M. B. Figueirêdo, P. J. Deuss, R. H. Venderbosch, H. J. Heeres, *ACS Sustainable Chem. Eng.* **2019**, *7*, 4755.

[44] M. B. Figueirêdo, H. J. Heeres, P. J. Deuss, *Sustainable Energy Fuels* **2020**, *4*, 265.

[45] M. B. Figueirêdo, F. W. Keij, A. Hommes, P. J. Deuss, R. H. Venderbosch, J. Yue, H. J. Heeres, *ACS Sustainable Chem. Eng.* **2019**, *7*, 18384.

[46] S. K. Tanneru, P. H. Steele, *Fuel* **2014**, *133*, 326.

[47] S. K. Tanneru, P. H. Steele, *Fuel* **2015**, *154*, 268.

[48] Y. Luo, V. K. Guda, E. B. Hassan, P. H. Steele, B. Mitchell, F. Yu, *Energy Convers. Manage.* **2016**, *112*, 319.

[49] S. K. Tanneru, P. H. Steele, *Renewable Energy* **2015**, *80*, 251.

[50] O. J. Guerra, J. Eichman, J. Kurtz, B.-M. Hodge, *Joule* **2019**, *3*, 2425.

[51] G. Glenk, S. Reichelstein, *Nat. Energy* **2019**, *4*, 216.

[52] J. A. Turner, *Science* **2004**, *305*, 972.

[53] H. Kawamoto, *J. Wood Sci.* **2017**, *63*, 117.

[54] R. A. Fenner, J. O. Lephardt, *J. Agric. Food Chem.* **1981**, *29*, 846.

[55] T. Han, N. Sophonrat, P. Evangelopoulos, H. Persson, W. Yang, P. Jönsson, *J. Anal. Appl. Pyrolysis* **2018**, *133*, 162.

[56] Q. Liu, S. Wang, Y. Zheng, Z. Luo, K. Cen, *J. Anal. Appl. Pyrolysis* **2008**, *82*, 170.

[57] R. Bayerbach, D. Meier, *J. Anal. Appl. Pyrolysis* **2009**, *85*, 98.

[58] C. Crestini, H. Lange, M. Sette, D. S. Argyropoulos, *Green Chem.* **2017**, *19*, 4104.

[59] J. Gierer, *Wood Sci. Technol.* **1980**, *14*, 241.

[60] A. Smit, W. Huijgen, *Green Chem.* **2017**, *19*, 5505.

[61] J. Sameni, S. Krigstin, M. Sain, *BioResources* **2017**, *12*, 1548.

[62] C. Schuerch, *J. Am. Chem. Soc.* **1952**, *74*, 5061.

[63] S. K. Tanneru, D. R. Parapati, P. H. Steele, *Energy* **2014**, *73*, 214.

[64] S. Zhang, T. Liu, C. Hao, L. Wang, J. Han, H. Liu, J. Zhang, *Green Chem.* **2018**, *20*, 2995.

[65] M. Ragnar, T. Eriksson, T. Reitberger, P. Brandt, *Holzforschung* **1999**, *53*, 423.

[66] S. Bezergianni, in *Liquid, Gaseous and Solid Biofuels – Conversion Techniques* (Ed: Z. Fang), InTech, London, UK **2013**, Ch. 9.

[67] D. C. Elliott, *Energy Fuels* **2007**, *21*, 1792.

[68] A. Panneerselvam, R. R. Sharma-Shivappa, P. Kolar, T. Ranney, S. Peretti, *Bioresour. Technol.* **2013**, *148*, 242.

[69] H. Prajitno, R. Insyani, J. Park, C. Ryu, J. Kim, *Appl. Energy* **2016**, *172*, 12.

[70] D. A. Ruddy, J. A. Schaidle, J. R. F. Iii, J. Wang, L. Moens, J. E. Hensley, *Green Chem.* **2014**, *16*, 454.

[71] J. Schulz, F. Bandermann, *Chem. Eng. Technol.* **1994**, *17*, 179.

[72] A. G. Gayubo, A. T. Aguayo, A. Atutxa, R. Aguado, J. Bilbao, *Ind. Eng. Chem. Res.* **2004**, *43*, 2610.

[73] S. Agarwal, D. van Es, H. J. Heeres, *J. Anal. Appl. Pyrolysis* **2017**, *123*, 134.

[74] T. P. Vispute, H. Zhang, A. Sanna, R. Xiao, G. W. Huber, *Science* **2010**, *330*, 1222.

1900147 (12 of 13)

**ADVANCED
SCIENCE NEWS**

www.advancedsciencenews.com

**ADVANCED
SUSTAINABLE
SYSTEMS**

www.advsustainsys.com

[75] G. W. Huber, A. Corma, *Angew. Chem., Int. Ed.* **2007**, *46*, 7184.

[76] Y. Wang, S. Agarwal, A. Kloekhorst, H. J. Heeres, *ChemSusChem* **2016**, *9*, 951.

[77] J. Bredenberg, M. Huuska, J. Räty, M. Korpio, *J. Catal.* **1982**, *77*, 242.

[78] M. B. Figueirêdo, Z. Jotic, P. J. Deuss, R. H. Venderbosch, H. J. Heeres, *Fuel Process. Technol.* **2019**, *189*, 28.

[79] P. Panagiotopoulou, D. I. Kondarides, X. E. Verykios, *J. Phys. Chem. C* **2011**, *115*, 1220.

[80] A. Friedl, E. Padouvas, H. Rotter, K. Varmuza, *Anal. Chim. Acta* **2005**, *544*, 191.

[81] A. Demirbas, *Energy Sources, Part B* **2007**, *2*, 311.

[82] G. W. Huber, R. D. Cortright, J. A. Dumesic, *Angew. Chem., Int. Ed.* **2004**, *43*, 1549.

[83] C. Mukarakate, R. J. Evans, S. Deutch, T. Evans, A. K. Starace, J. ten Dam, M. J. Watson, K. Magrini, *Energy Fuels* **2017**, *31*, 1600.

[84] B. M. Wagenaar, W. Prins, W. P. M. van Swaaij, *Chem. Eng. Sci.* **1994**, *49*, 5109.

[85] M. B. Figueirêdo, P. J. Deuss, R. H. Venderbosch, H. J. Heeres, *Biomass Bioenergy* **2020**, *134*, 105484.

1900147 (13 of 13)